ANNALS OF GEOPHYSICS, 66, 3-4, SE319, 2023; doi:10.4401/ag-8950
OPEN ACCESS

Geophysical and geological signatures of an unknown fault in the historic center of Messina (Sicily, south Italy)

Paolo Pino[1,2], Silvia Scolaro[*,1,2], Antonino Torre[1,2], Sebastiano D'Amico[3], Giancarlo Neri[2] and Debora Presti[2]

(1) Department of Engineering, University of Messina
(2) Department of Mathematics, Computer Sciences, Physics, and Earth Sciences, University of Messina
(3) Department of Geosciences, University of Malta

Article history: received February 13, 2023; accepted June 26, 2023

Abstract

Analysis of seismic noise measurements shows a clear change of the Site Resonant Frequency across a NW-SE segment cutting the historic center of the town of Messina. This change indicates strong lateral heterogeneity of the sediment cover going from southwest to northeast across the segment and suggests the existence of a fault never reported by previous investigators, oriented differently from the NNE-SSW main structural system which is widely believed to have produced the magnitude 7.1 earthquake of 1908. Additional evidence of such a NW-SE fault has been obtained by surface geology and analysis of morphological and Digital Terrain Model data. Geologic observations clearly indicate normal faulting but are not able to identify eventual strike-slip components. Activity of this fault is documented at least until Middle Pleistocene based on stratigraphic evidence and borehole data, with likely prosecution during Upper Pleistocene. The new detected fault requires deeper investigation in the near future for evaluation of its real extent and present dynamics including eventual seismogenic attitude.

Keywords: Faults; Seismic noise measurements; Surface geology; Digital Terrain Modeling; Messina

1. Introduction

Taking benefit from a database of HVSR (Horizontal-to-Vertical Spectral Ratio) measurements obtained by seismic noise campaigns performed in the town of Messina over the last years [Scolaro et al., 2018; Neri et al., 2022; Municipality of Messina, 2014; Di Nuzzo personal communication], integrated by new measurements performed in the present study, we may analyze lateral variations of the sedimentary cover beneath the center of the town. Joining this geophysical analysis with geological and geomorphological observations also made in the present study, we attempt to identify structural discontinuities and faults which may, among other things, represent sources of hazard in a town well known to be exposed to very high seismic risk.

The efforts made in the present study have allowed us to detect a previously undocumented fault, crossing the center of the town from NW to SE and therefore referable to the structural system NW-SE reputed of minor relevance by several authors [e.g., Ghisetti and Vezzani, 1982; Ghisetti, 1984, 1992; Monaco and Tortorici 2000], who highlighted the major role of the NNE-SSW structural system in the whole Straits area (see next paragraph). We here attempt a preliminary characterization of the new detected fault and a first approach to the exploration of possible relationships between this fault and the local seismicity. Even considering the widely shared major role of the NNE-SSW structural system as source of strong earthquakes in the Messina Straits area [e.g., Boschi et al., 1989; Neri et al., 2006; DISS Working Group, 2021], we do believe that exploring other structural systems (such as the NW-SE one) also in terms of seismic potential may be appropriate. The largely prevailing (if not exclusive) attention paid to date by the scientific community towards the source of the 1908 earthquake has produced the effect of limiting the efforts for the seismological characterization of other structures, such as, in particular, the NW-SE structural system.

2. Geostructural and geodynamic features of the study area

Messina city is located on the Sicilian side of Messina Straits, a narrow graben-like, fan-shaped tectonic depression transverse to the Calabro-Peloritan Arc [Figure 1a; Selli, 1979; Ghisetti, 1992; Amodio Morelli et al., 1976]. The Messina Straits, originated from Upper Pliocene and currently subsiding [Selli, 1979; Barrier, 1986; Ghisetti, 1992; Lentini and Carbone, 2014], represents the main tectonic system of this region [Monaco and Tortorici, 2000; Finetti et al., 2005; Catalano et al., 2008], characterized by an extensional stress directed ESE-WNW [Tortorici et al., 1995; Neri et al., 2004 and 2005; Presti et al., 2013; Totaro et al., 2016; Mariucci and Montone, 2020].

The Messina Straits is dominated by NNE-SSW and NE-SW structural systems [Figure 1b; see also Ghisetti, 1979, 1984, 1992; Monaco and Tortorici, 2000]. In the Messina area (Figure 2) the NNE-SSW structural system consists of ESE-dipping normal faults showing an en-echelon and step-shaped pattern, running parallel to the coastline [Ghisetti, 1984 and 1992]. The major faults belonging to this NNE-SSW structural system are Larderia-Curcuraci, boarding with evident scarps the NE Peloritan Ridge where metamorphic paleozoic basement is strongly uplifted [Figure 2; Ghisetti, 1992] and Messina-Fiumefreddo, drawing the current Ionian coastline from Grotte locality (north of Messina city) to Fiumefreddo-Giarre, on the eastern slope of Etna volcano (Figure 1). This structural setting is commonly accepted in the literature [Gargano, 1994; Lentini, 1999; Servizio Geologico di Italia, 2008] and reconstructed also below the Olocene coastal alluvial plain deposits, where significant vertical displacements attributable to normal faults were deduced from deep borehole and geophysical data [Ferrara, 1999].

The most recent age of activity of NNE-SSW faults dates back to the upper Pleistocene, proven by geological field data, as they cross-cut the middle-Pleistocene clastic deposits of the Messina Formation. The NNE-SSW fault system is intersected by ESE-WNW and ENE-WSW normal faults which steeply bound several transverse horst-like structures, strongly uplifted in Pleistocene times [Ghisetti, 1984]. This process can, for example, be observed in the area of the Ganzirri-Scilla System (Figure 2) where the north-eastern termination of the Straits appears rotated to N70°E forming Capo Peloro [Guarnieri et al., 2004]. The Ganzirri horst is bordered on the northern side by the arched WNW-ESE Mortelle fault [Ghisetti, 1992] and on the southern side by the Granatari fault [Figure 2; Ghisetti, 1992]. Another example of transverse horst originated by the ENE-WSW fault system can be found near the harbor of Messina (La Falce; Figure 2), as suggested by sea-bottom morphology and the presence of a cristalline outcrop [Franchi, 1909; Ghisetti, 1984]. The ENE-WSW system cuts the NNE-SSW one and therefore appears to be more recent, even if it cannot be excluded that the more recent faults may merge into it with its reactivation [Gargano, 1994; Lentini et al., 1999]. In the immediate offshore of northern Messina, a blind normal fault with the same trend, named Messina Straits Fault, has been detected by seismic reflection data [Figure 2; Doglioni et al., 2012]. Six orders of marine terraces recognized on the Capo Peloro promontory aged from 60 to 240 ka are tilted of ~10-15° southward due to the activity of the Mortelle Fault [Figure 2; Monaco et al., 2017].

Structural data of the Straits marine area [Selli et al., 1978] evidence the presence of N-S, E-W and NW-SE trending lineaments. The NW-trending faults belonging to the South-Tyrrhenian System and responsible of the right lateral shifting of the entire orogenic chain [Lentini et al. 1994; Finetti et al. 1996] do not appear to be much developed onshore, even if some seismic lines show images of flower-like structures linked to NW-oriented strike-slip faults with dextral component [Del Ben et al., 1996]. As a consequence, in the geological maps and literature this structural trend is nearly absent on the Sicilian coastal belt of the Straits [Ghisetti, 1984, 1992; Gargano, 1994;

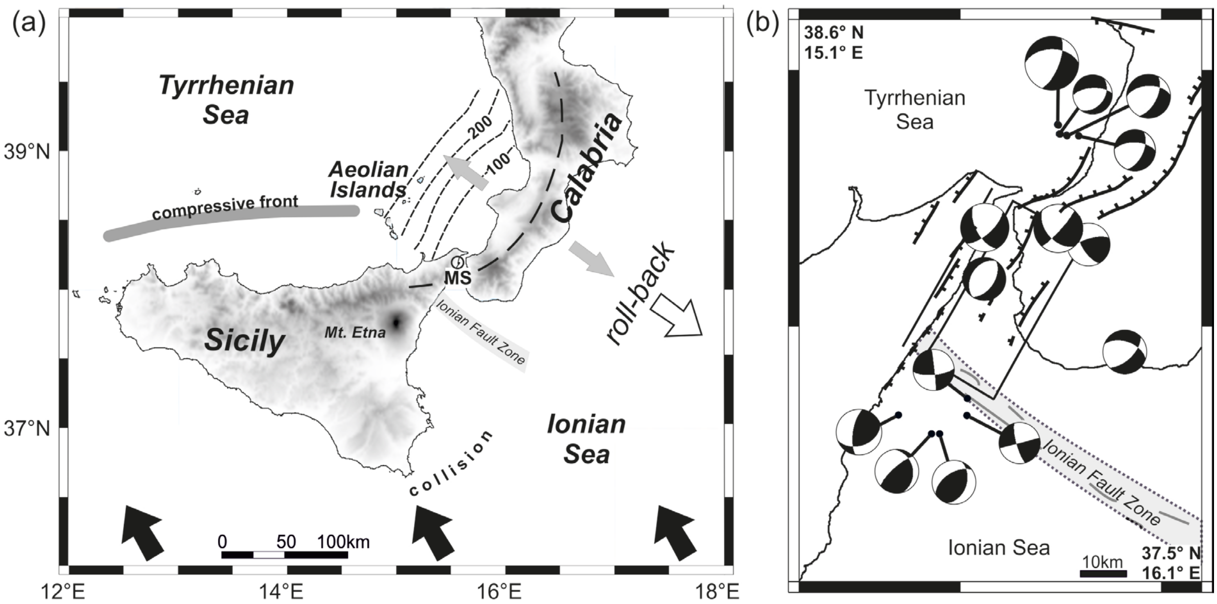

Figure 1. (a) Map view of the Southern Tyrrhenian region. The dashed curved line indicates the mountain chain of the Calabro-Peloritan Arc. The black arrows in the bottom of the figure indicate the present motion of Nubia relative to Eurasia [Nocquet, 2012, and references therein]. The white arrow shows the sense of rollback of the Ionian subducting slab. The gray divergent arrows indicate the direction of extension according to stress estimates [Tortorici et al., 1995; Totaro et al., 2016]. Dashed lines between Calabria and the Aeolian Islands are depth contour lines of the Wadati-Benioff zone [Faccenna et al., 2011]. The SE-striking gray belt in the Ionian Sea shows the location of the Ionian Fault Zone [see Polonia et al., 2016, among others]. MS stands for Messina Straits area, the small circle indicates the location of the town of Messina. (b) Enlarged view of the Messina Straits area showing the main fault systems [Ghisetti et al., 1984; Monaco and Tortorici, 2000] and the waveform inversion focal mechanisms [from Neri et al. 2021] indicating the transitional character of the Messina Straits area between extensional and compressional domains (see text for details). The SE-striking gray belt in the Ionian Sea shows the location of the Ionian Fault Zone [Polonia et al., 2016, among others]. Rectangle and line refer to the 1908 earthquake source and represent, respectively, the surface projection of the seismic source (DISS Working Group, 2021) and the intersection between the source prolongation and the surface.

Lentini, 1999]. In this connection, the only structure attributable to this system could be the “Pantano Piccolo fault” [Figure 2; Ghisetti, 1984], that cuts the end of the Ganzirri peninsula, favoring the origin of the “Pantano Piccolo” lake. This trend seems to abruptly interrupt the Mortelle and Granatari faults, in the easternmost termination of the Capo Peloro promontory. It is possible that the NW-SE system is more recent than the Mortelle fault certainly active in the late Pleistocene (<60 ka). As reported in Selli et al. [1978], the NW-SE faults are mainly submarine, many of them appear on the bottom of the Straits where they cross and sometimes displace the E-W and N-S ones. Finally, west of the Ganzirri lake, another fault lineament, oriented between N-S and NNW-SSE, has been hypothesized on a morphological basis within the sands and gravels Messina Formation between the village of Faro Superiore and the Papardo valley [Guarnieri and Pirrotta, 2008]. This structure (see Fault 5 in Figure 2) has been identified as a strike-slip right-lateral fault and it probably continues southward offshore in front of Messina city [Finetti, 2008].

All the above mentioned fault systems seem to have participated simultaneously in the dynamics of the area, with variable displacements, even with secondary accomodation, at least until after the uppermost Pleistocene, but it cannot be excluded that this simultaneous action of the various fault systems is currently active [Selli 1979; Guarnieri et al., 2004; Guarnieri and Pirrotta 2008].

In a very recent geodynamic reconstruction by Neri et al. [2021] the Messina Straits area is transitional between (Figure 1) the zone of rollback of the in-depth continuous Ionian subducting slab (southern Calabria) and the collisional zone where the subduction slab did already undergo detachment (southwest of the Ionian fault zone). Normal faulting earthquakes in the Tyrrhenian sea offshore southern Calabria (Figure 1) are compatible with southeast-ward rollback and trench retreat of the subducting Ionian slab. Reverse mechanisms in the Ionian sea

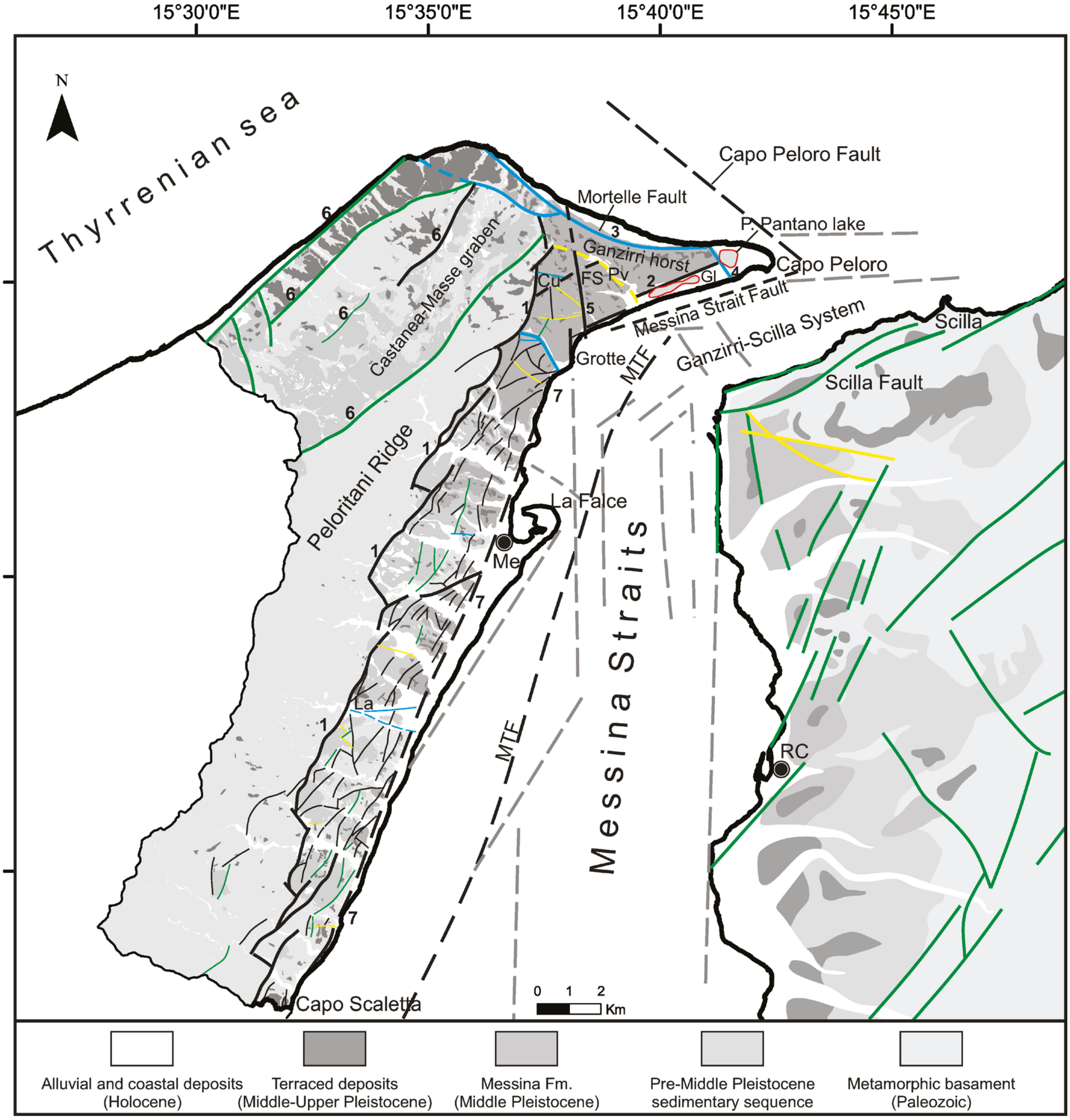

Figure 2. Simplified structural map of the Messina Straits area. Fault legend: 1 NNE-SSW Curcuraci-Larderia Fault System [Ghisetti, 1992]; 2 ENE-WSW Granatari Fault [Ghisetti, 1992]; 3 E-W Mortelle Fault [Ghisetti, 1992]; 4 NW-SE Pantano Piccolo Fault [Ghisetti, 1992]; 5 NNW-SSE Faro Superiore Fault [Guarnieri e Pirrotta, 2008]; 6 NE-SW trending faults [Ghisetti, 1992]; 7 Capo Scaletta-Grotte Fault [Selli, 1979]. MTF: Messina-Taormina Fault [Doglioni et al., 2012; Meschis et al., 2019]. Capo Peloro Fault and Messina Strait Fault from Doglioni et al. [2012], Ganzirri-Scilla System from Guarnieri et al. [2004], Scilla fault from Ferranti et al. [2008]. Black lines: E-dipping normal faults; blue lines: N-dipping normal faults; yellow lines: S-dipping normal faults; green lines: W-dipping normal faults. The fairly dense network of grey-dashed lines represents offshore faults [Selli, 1979; Guarnieri et al., 2004]. Thinner lines indicates minor faults mainly belonging to the en-echelon NNE-SSW system n. 1. Dashed lines: inferred faults. Gl: Ganzirri lake; Pv: Papardo valley; FS: Faro Superiore village; Cu: Curcuraci village; La: Larderia village; Me: Messina city center; RC: Reggio Calabria city center.

southwest of the Ionian fault zone (Figure 1) are compatible with the collisional domain existing southwest of the subducting slab edge. The transitional character of the Messina Straits implies reasonably the coexistence of normal and strike-slip faulting (Figure 1).

The magnitude 7.1 earthquake of 28 December 1908 is the strongest earthquake occurred in the Messina Straits area in historic times [Rovida et al., 2022]. The search for the source of this earthquake has engaged scientists for several decades. After the first paper by Schick [1977], tens of papers have been published reporting different hypotheses as regard to location, strike and dip of the fault which generated the event, with normal faulting mechanism substantially shared by all models, however. Circa N-striking east-dipping faults with top located beneath the Sicilian side of the Messina Straits area were proposed by many authors [Amoruso et al., 2002 and 2006; DISS Working Group, 2021], while west-dipping sources with top beneath the Calabrian side were preferred by Bottari et al. [1986] and Aloisi et al. [2013]. Today, on the basis of the wide debate which has developed in the literature, the largely most convincing source of the 1908 earthquake appears to be a low-angle east-dipping normal fault striking between N10W and NNE, with the top located a few km beneath the Sicilian side of the Straits [Figure 1b. Capuano et al., 1988; Boschi et al., 1989; De Natale and Pingue, 1991; Amoruso et al., 2002; DISS Working Group, 2021]. It is worth mentioning that analogue modelling allowed Bonini et al. [2011] to state that high-angle, outcropping normal faults observed over all the Messina Straits area can be interpreted as minor structures related to the activity of this low-angle east-dipping, deeper normal fault believed to have generated the 1908 earthquake. In very recent times, new debate on the 1908 earthquake source has been stimulated by a paper by Barreca et al. [2021], proposing a NNE-trending SE-dipping fault in the Messina Straits with NE-ward rotation at its northernmost part and possible continuation across southern Calabria mainland, and concerned comments by Pino et al. [2021] and Argnani [2022].

3. Data, analysis and results

3.1 Seismic Noise: Horizontal-to-Vertical Spectral Ratio

The HVSR (Horizontal-to-Vertical Spectral Ratio) method is based on the computation of the Fourier spectra of the three components of the ambient seismic noise, and the estimate of the spectral ratio between the average of the horizontal components (H) and the vertical one (V) [Nogoshi and Igarashi, 1971; Nakamura, 1989]. The ambient noise wavefield is a combination of both body and surface waves, and the fundamental frequency peak in the spectral ratio can be interpreted both in terms of SH resonance in superficial layers and ellipticity if Rayleigh surface waves predominate [Fäh et al., 2001; Bonnefoy-Claudet et al., 2006a]. The HVSR method allows to identify the fundamental frequency f_0 corresponding to the resonance frequency that is in turn controlled by the sedimentary layer thickness [Nakamura, 1989; Lachet and Bard, 1994; Ibs-von Seht and Wohlenberg, 1999; Bonnefoy-Claudet et al., 2006a and 2006b; Castellaro and Mulargia, 2009; Di Giulio et al., 2016].

In the present study, we have performed new single-station ambient noise measurements and have integrated the HVSR database built through previous surveys carried out in the town of Messina (Figure 3; Municipality of Messina, 2014; Scolaro et al., 2018; Neri et al., 2022; Di Nuzzo personal communication). We have used two different portable sensors: the short-period, 3-component digital seismometer Tromino (https://moho.world/tromino/) and the broadband, 3-component digital seismometer GEOtiny (https://geobit-instruments.com/). Both instruments have been used simultaneously at the same site for 60 minutes of recording with a sampling rate of 256 Hz. The data have been analyzed by Grilla (https://moho.world/tromino/) and Geopsy [Wathelet et al., 2020; http://www.geopsy.org] software, following the SESAME guidelines [Bard, 2005]. Each recorded time history has been divided into non-overlapping time windows 40 s long. The Fourier spectrum of each time window has been calculated and smoothed through a triangular smoothing function with a width equal to 5% the central frequency. The HVSR spectral ratio has been computed for each frequency by (i) averaging the horizontal spectra using the geometrical mean and (ii) dividing this average value by the vertical spectrum, for each time window. Before interpreting the resulting HVSR curves, the data have been controlled to exclude transient disturbances from nearby sources (e.g., due to impulsive or strongly localized anthropic sources). The analyses have been limited to the frequency range 0.1-20 Hz containing the frequency band of 0.4-10 Hz in which the main contribution from the local geological structures is expected.

Examples of HVSR curves obtained at two different sites by Tromino and GEOtiny sensors are displayed in Figure 4, where a good match between the Tromino and GEOtiny curves can be appreciated. Focusing our attention on the site fundamental frequency f_0, all the available HVSR curves show the peak in the range between 0.4 Hz and 1.6 Hz (Figure 5). The wide set of available ambient noise measurements allows us to detect a clear drop of

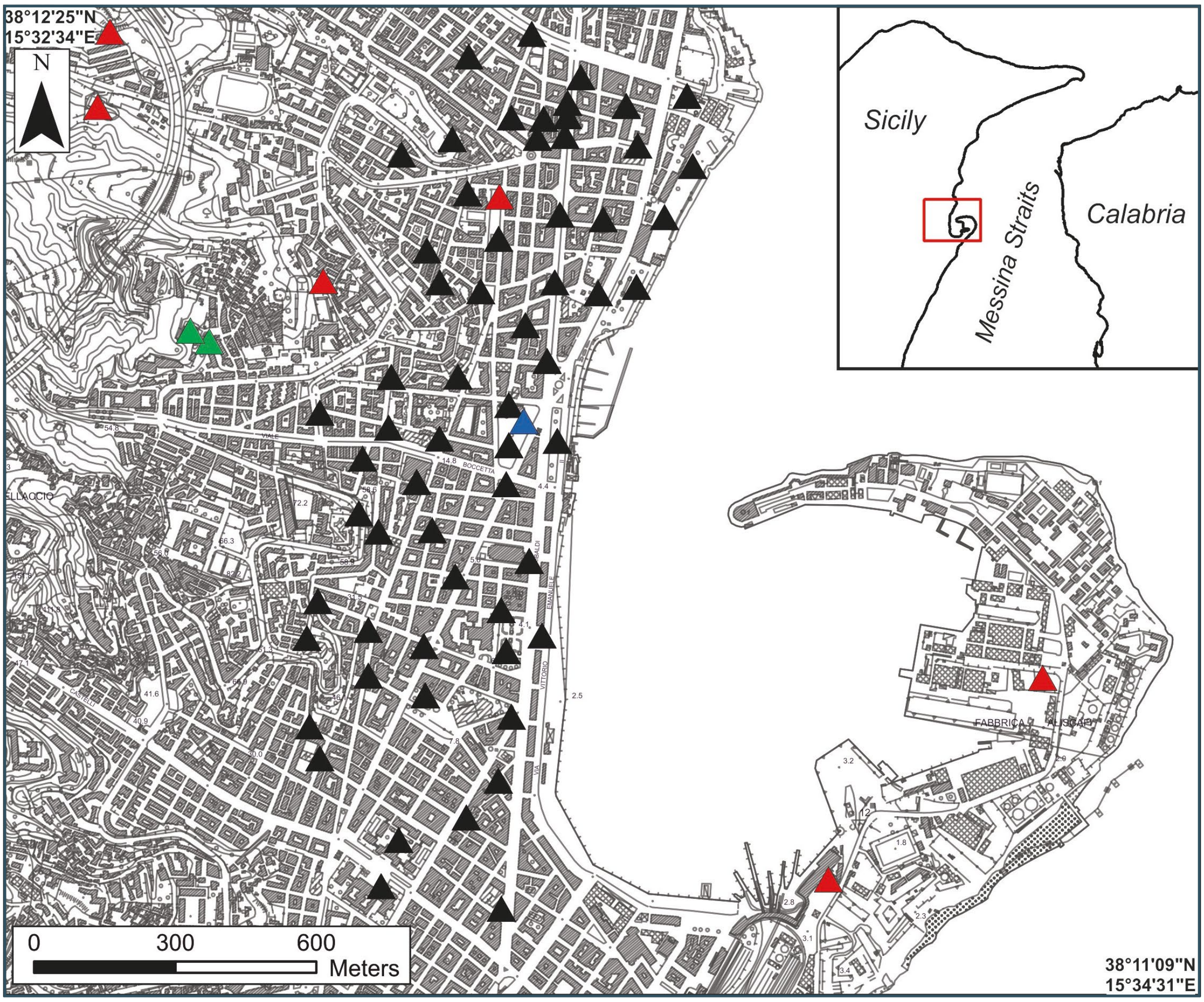

Figure 3. The figure shows the topographic map 1:10.000 of the historic center of Messina (red rectangle in the top-right inset) with triangles indicating the location of the HVSR measurement stations (red: present study; black: Scolaro et al., 2018 and Neri et al., 2022; green: Di Nuzzo, personal communication; blue: Municipality of Messina, 2013). HVSR data from Municipality of Messina (2013) consist of five measurements very close in space with identical results that, for graphical reasons, are here indicated by a single blue triangle.

the fundamental frequency f_0 moving northeast-ward across a circa NW-trending segment located just in the historic center of the town of Messina (dashed segment in Figure 5). f_0-values in the range 0.4-0.7 Hz can be mainly observed in the northeastern sectors of the investigated area, higher values between 0.7 and 1.6 Hz are detected in the southwestern sector. The spatial pattern of HVSR peak frequencies f_0 in Figure 5 evidences a strong lateral heterogeneity in the stratigraphy beneath the center of the town, in correspondence of the already mentioned NW-trending segment. In the framework of a project funded by Sicily Region (P.O. FESR SICILIA 2014/2020, 08CT2790090212) we are currently planning a new series of geophysical measurements (HVSR, seismic arrays and resistivity profiles) aimed to deepen the knowledge of this discontinuity zone and to explore a possible prosecution of it beyond its presently detected northwestern and southeastern edges. In this connection, it can be noted that only two HVSR data are available in the "La Falce" area, southeast of the detected NW-trending discontinuity. These data do not seem to fit the pattern of data (high vs low frequencies) observed in the center of the town, once the NW-trending discontinuity is supposed to prosecute southeastward. In particular, low frequency obtained at the southern point of measurement in the "La Falce" area apparently contrasts with the high frequency domain expected on the footwall of the NW-trending fault. In any case, more data are needed to better define the structural scenario in this coastal sector, also considering the diffused presence here of NNE-trending faults (Figure 2) and possible interactions of these with our NW-trending fault.

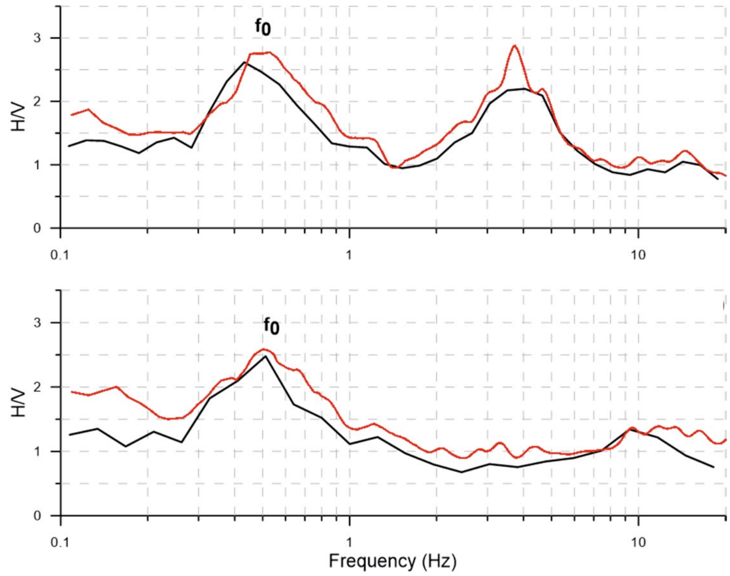

Figure 4. Two examples of comparison at different sites between HVSR curves obtained using Tromino (red line) and GEOtiny (black line). f_0 indicates the site fundamental frequency.

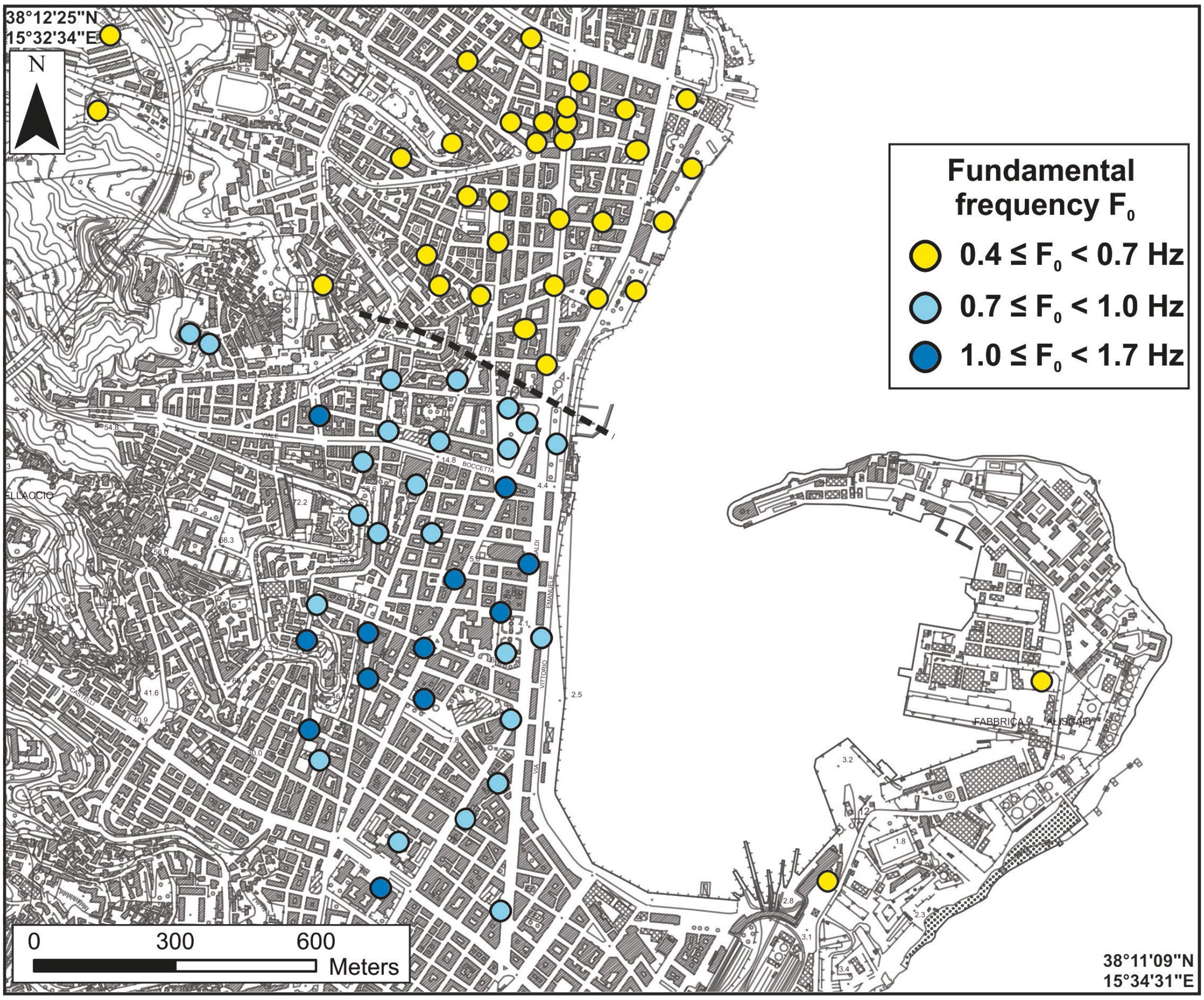

Figure 5. Topographic map 1:10.000 of the historic center of Messina with the spatial distribution (colored circles) of the site fundamental frequencies f_0 available in the present study (see legend). The f_0 values evidence a strong lateral variation of stratigraphy across a circa NW-trending segment (dotted black line). This transition of the fundamental frequency was, at some extent, already visible in the plots of Scolaro et al. [2018] but it was not discussed nor explicitly presented there. In our map, the use of a larger dataset and of different frequency partitions (implying a different color scale) allows for better detection of the lateral discontinuity, what helps fruitful comparison with geological and geomorphological data.

3.2 Geology and geomorphology

In the present study, we investigate the possible presence of a NW-SE fault (hereafter Trapani Stream Fault) along the peri-coastal sector of Messina city, roughly corresponding to the valley of Torrente Trapani (Figure 6), which could be responsible of the sharp fall in the values of f_0 evidenced by the analysis of the HVSR database in the sub-section 3.1 (Figure 5). In the study area the tectonics has a strong influence on the shapes of the landscape and a valid interpretative support can be provided by analysis of satellite images, contour lines in the topographic maps and DTM (Digital Terrain Model) data.

We started this investigation with the analysis of cartographic data at 1:10.000 and 1:2.000 scales, furnished by Regione Siciliana (www.sitr.regione.sicilia.it) and Messina Municipality, respectively. From this analysis, we have found straight slopes with trapezoidal/triangular facets aligned. At the scale 1:2.000, the trapezoidal/triangular facets are more evident in the innermost sector investigated in the Torrente Trapani valley (Figure 6), while less clear morpho-structural evidences are found along the more coastal slopes where urbanization is strong. These morpho-structural evidences of the Trapani Stream Fault have been confirmed directly on field (Figure 6).

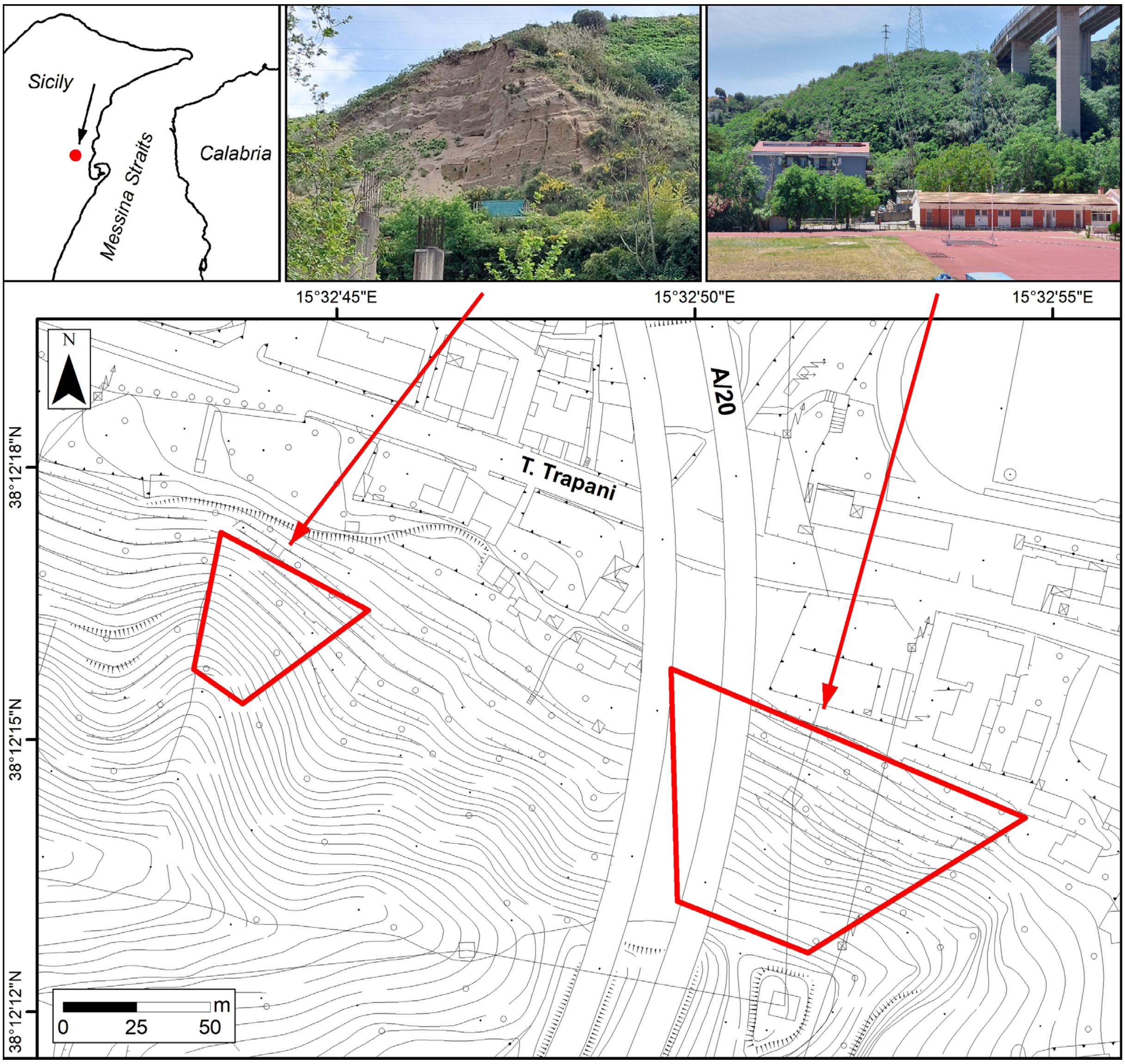

Figure 6. The main plot shows two trapezoidal slopes aligned in the NW-SE direction in the T. Trapani valley near A/20 highway (topographic map 1:2.000 furnished by Messina Municipality). The top-left plot shows the Messina Straits area, with indication of the location area of trapezoidal slopes. The two pictures show the trapezoidal slopes shaped in gravels and sands of Messina Formation.

Both in the cartographic maps and in the field analyses, evident morpho-structures alternate with concave stretches of slope referred to areas subjected to more intense erosive and gravitational modeling processes. In fact, the slope basis is often covered by eluvium-colluvial deposits and talus slope that contribute to smoothing slopes and to morphological patterns of the land nearby. This is a normal consequence because the rock types in the study area are represented by moderately thickened gravels and gray-yellowish and orange-brown sands, sometimes with a variable and subordinate silty component, substantially uniform and erodible (see pictures in Figure 6). These lithological units are attributable to the Middle-Pleistocene Formation "Ghiaie e Sabbie di Messina" [see, e.g., Gargano, 1994; Lentini et al., 1999, 2000; Servizio Geologico d'Italia, 2008], which forms the backbone of the hills overlooking the coastal plain of Messina city center. They are closed at the top by Late-Middle Pleistocene – Upper Pleistocene terraced fluvial-marine deposits, while in the valley floor there are current alluvial deposits.

Detailed geological surveys have been conducted in the present study in a large area around the valley of Torrente Trapani (Figure 7a), in order to define the stratigraphic-structural nature at the basis of the strong lateral heterogeneity revealed by the marked variation of the HVSR fundamental frequency (Figure 5). During our geological surveys in the innermost sector of Torrente Trapani at the base of the morpho-structured slope (Figure 6), we have found the geological boundary between the gravelly-sandy succession (Messina Formation) and the underlying whitish marly limestones (Trubi Formation, Figure 8a). These marly limestones (Figure 8b) have been attributed to Trubi Formation of the lower Pliocene [see, e.g., Gargano, 1994; Lentini et al., 1999; 2000; Servizio Geologico d'Italia, 2008], which has often been recognized in the area of Messina as a geological substratum of Ghiaie e Sabbie di Messina Formation, clearly in unconformity contact [Bonfiglio et al. 1991; Lentini et al., 2000]. The geological maps [Gargano, 1994; Lentini et al., 1999] highlight also overlaps of Messina Formation directly on late Miocene siliciclastic succession of San Pier Niceto Formation [Servizio Geologico d'Italia, 2008]. Our new geological surveys have evidenced a considerable structural fragmentation and strong stratigraphic gaps mainly due to extensional faults, with lithostratigraphic sequences almost never continuous, both vertically and laterally (Figure 7a).

The most recent official review of the Messina geological map [Servizio Geologico d'Italia, 2008] does not include our study sector. However, chronostratigraphic updating of the various geological formations and their nomenclature, recently introduced by CARG-project [Servizio Geologico d'Italia, 2008], have been used in the present study (Figure 7a). The Ghiaie e Sabbie di Messina Formation, overlapped by terraced fluvial-marine deposits, can be found on the opposite side of the valley on the hydrographic left of Torrente Trapani, in accordance with the known geology of Messina [Gargano, 1994; Lentini et al., 1999]. Therefore, the emergence of Messina Formation substrate at the altitude of at least 6 meters, with respect to the valley floor of Torrente Trapani, can be justified by a fault (Trapani Stream Fault) inside the valley of Torrente Trapani, responsible for the lowering of the stratigraphic series towards NNE (Figure 7b).

The Trapani Stream Fault, buried by the current alluvial deposits and by continental debris on the slope, is confirmed by the results of a geognostic borehole carried out on the Torrente Trapani valley floor, at a distance of about 30 m from the site of Figure 8 and with a difference in altitude of 6 meters (Figure 7b). The borehole, named S455 [Società Stretto di Messina, 2011], reached a total depth of 60 meters and intercepted the geological contact between clastic deposits (Ghiaie e Sabbie di Messina Formation) and whitish calcareous marl (Trubi Formation) at 17 meters of depth beneath the ground level of the Torrente Trapani valley floor. This stratigraphy shows a dislocation of the stratigraphic limit between Messina Formation and Trubi Formation, with a displacement of at least 23 meters over a horizontal distance of 30 meters, justifiable by the activity of a normal or transtensive fault. The borehole data near the southwestern edge of the valley floor, lead us to consider that the thickness of alluvial deposits overlaying the clastic deposits of Messina Formation (Figure 7b) is of the order of 5 meters. The location of the Trapani Stream Fault can be constrained between the borehole position (hanging wall) and the outcrop section of the Trubi Formation on the footwall. The proximity of the borehole to the fault, leads to the reasonable hypothesis that it may have partly sampled the lowered side (hanging wall) and partly the raised side (footwall) of the fault itself (Figure 7b). This could explain the small thickness of marly limestone of Trubi Formation (about 1.3 m) sampled by the borehole, compared to those observed on the raised side (at least 2.5 m). No evident sign has been found along the exposed wall, useful to define the kinematics of the fault (Figure 8c).

We have also studied the geomorphological features of the area of interest using the GIS analysis on 2m-resolution DTM provided by the Sicilian Region and created through post-processing of LIDAR data (https://map.sitr.regione.sicilia.it). In particular, we have processed the DTM data by the shaded relief tool, which allowed us to obtain a relief model of the study area (Figure 9). This process, through the use of simulated light, allows the observation of Earth's surface morphology with a better perception of the elevation, due to the 3D effect. It represents a valid

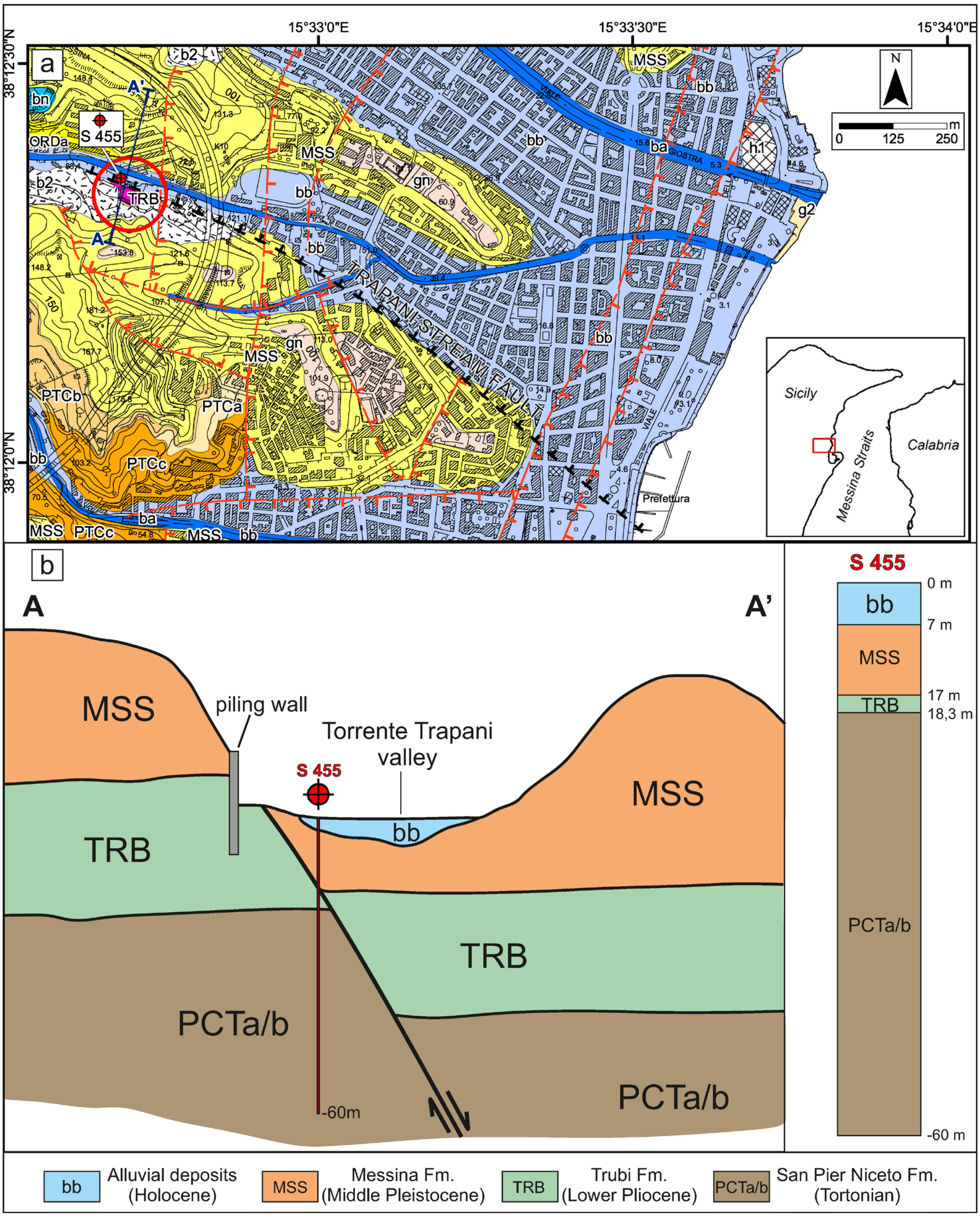

Figure 7. (a) New geological map of the northern sector of Messina city center, the location of which in the broader area is indicated in the inset. Red circle: survey and S 455 drilling site. Geological legend: h1: anthropic fill (Holocene); g2: coastal deposits (Holocene); b2: colluvial detrital deposits; ba and bb: alluvial deposits (Holocene); bn: fluvial terraces deposits (Holocene); gn: marine terraces deposits (Upper Pleistocene); MSS: gravel and sands of Messina Formation (Middle Pleistocene); ORDa: calcarenites of San Corrado Formation (Middle Pleistocene); TRB: White marls and marly limestones of Trubi Formation (Lower Pliocene); PTCa: dark gray clays of San Pier Niceto Formation (Tortonian); PTCb: sandstones low cemented light gray of San Pier Niceto Formation (Tortonian); PTCc: conglomerate slow cemented of San Pier Niceto Formation (Tortonian). Continued and dashed red lines: certain and inferred normal faults, respectively; black dashed line: Trapani Stream Fault detected in the present study; blue line (A-A'): trace of schematic geological section shown in plot (b); red dot: S455 borehole reported in plot (b) (see text for details). (b) Interpretative geological section of stratigraphy along the profile A-A' (Figure 7a) supported by field and borehole data (not in scale). Piling wall is the site shown in Figure 8. The schematic stratigraphic log of S455 borehole is reported on the right (Società Stretto di Messina, 2011).

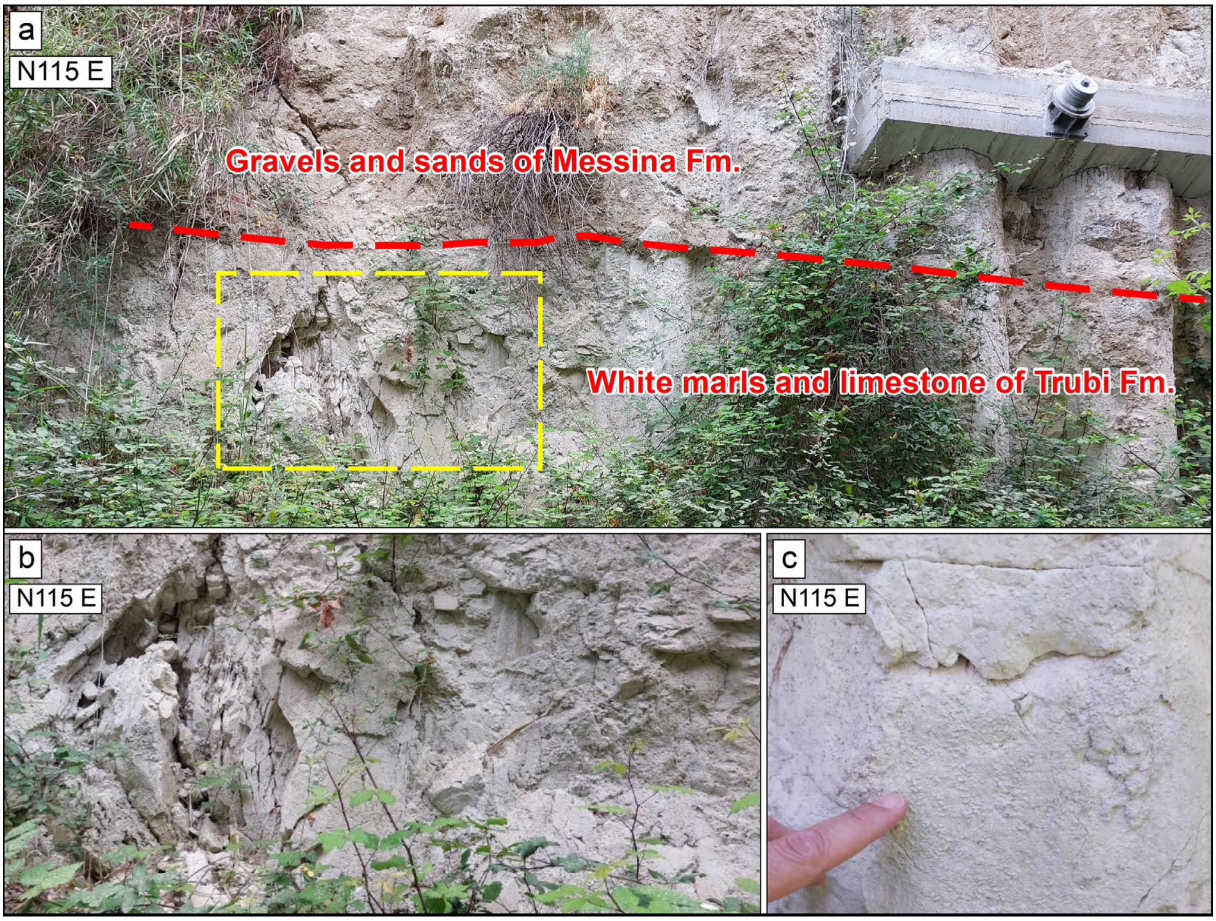

Figure 8. (a) Picture of the frontal view of the cut-slope localized within the red circle area in Figure 7a. We observe here the discordant stratigraphic contact (red dashed line) between the upper gravels and sands of the Messina Formation and the underlying marly limestones of the Trubi formation. The yellow box indicates the part of the picture shown enlarged in plot (b). (b) Zoom view of white marly limestones (Trubi Formation). (c) Fractures and joints system observed in the Trubi Formation, without clear evidence of kinematic indicators of faulting.

support in geomorphological analyses, integrating and supporting the field surveys. The shaded relief of Figure 9 clearly highlights the slope in the Torrente Trapani valley (northwestern branch of the morphological feature) and its prosecution in most of the urbanized coastal area (southeastern branch). In the latter, there are curved and hollow geomorphological forms, indicative of the erosive activity occurred over the time. Some dismantling and partial obliteration of the fault escarpment was certainly favored by remodeling made by human activity and probably by erosion activity carried out over time by the Trapani stream. We conclude that the fault segment found in the Torrente Trapani valley prosecutes southeast-ward into the coastal plain (Trapani Stream Fault), bordering the hills' basis representing the footwall, with WNW-ESE and NW-SE orientations in the northwestern and southeastern branches, respectively (Figure 9). The Trapani Stream Fault here detected is not reported in the official geological maps of the study area [Gargano, 1994; Lentini et al., 1999] and in the scientific literature [see, e.g., Ghisetti, 1984; 1992; Guarnieri et al., 2004; Guarnieri, 2006; Comerci et al., 2015].

The Trapani Stream Fault activity is certainly more recent than "Ghiaie e Sabbie di Messina" Formation which is dislocated by this fault and have an absolute age of 200 ± 40 ka [Bada et al., 1991; Bonfiglio et al., 1991]. Furthermore, at the top of Messina Formation there are various orders of marine abrasion surfaces and terraced fluvial-marine deposits, between 150 m a.s.l. and 35 m a.s.l., with an age of 200-60 ka, corresponding to the Marine Isotopic Stage MIS 7.1 (200 ka) and MIS 3.3 (60 ka), that are located at Capo Peloro [Catalano and De Guidi, 2003; Monaco et al., 2017] and in the Tyrrhenian side of the Municipality of Messina [Catalano and De Guidi, 2003; Catalano and Cinque, 1995]. Therefore, considering the morphological displacement between marine abrasion surfaces and terraced fluvial-marine deposits in the Torrente Trapani valley, it cannot be excluded that the activity of the Trapani Stream

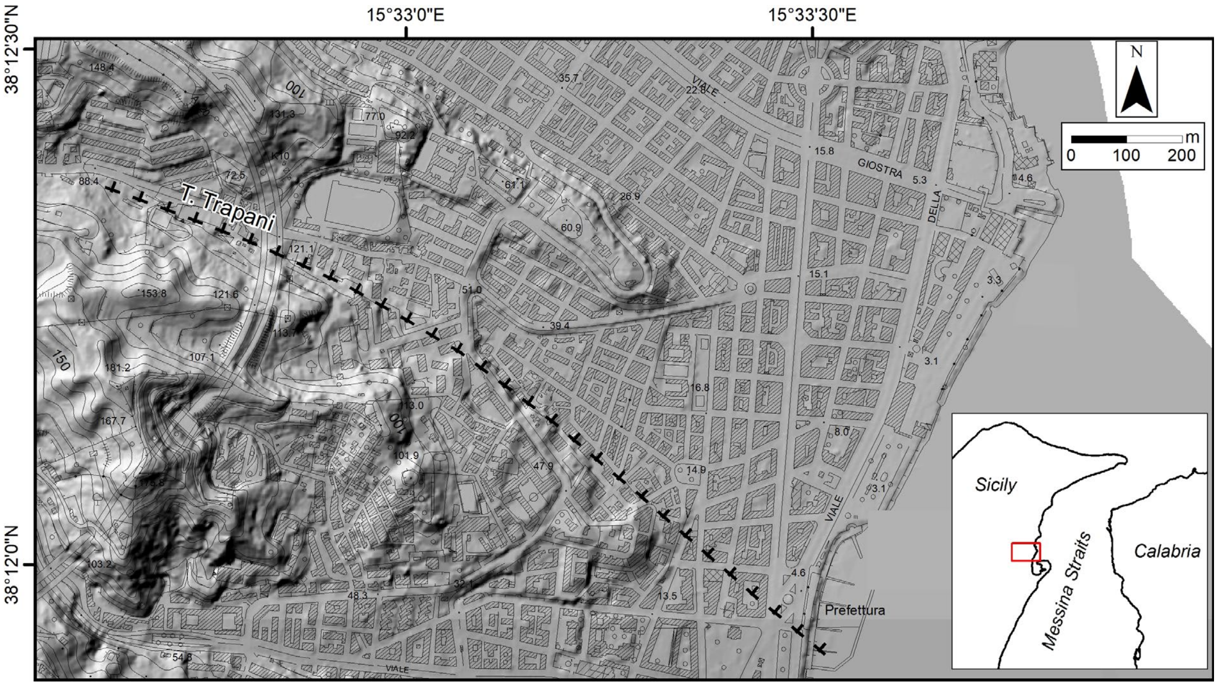

Figure 9. Shaded relief of the study area with indication of the Trapani Stream Fault (black dashed line) detected in the present study on the basis of geophysical (HVSR), geological and geomorphological evidences.

Fault is more recent than 60 ka. No other clear evidence of recent activity has been found. In fact, there are no geological sections emerging in the current continental deposits that cover the fault zone, and this has prevented us from finding any sign of current tectonic deformation.

4. Discussion and conclusion

The analysis of HVSR measurements highlights strong lateral heterogeneity of the sediment cover going from southwest to northeast in the historic center of the town of Messina (Figure 5). Such a clear change may suggest the existence of a NW-trending fault (Trapani Stream Fault), but no fault with that orientation is reported in the zone of the change in the existing geological maps [see, among others, Ghisetti, 1992; Gargano, 1994; Lentini et al., 1999]. The NW-SE trending structural system is widely considered of minor relevance in the Messina Straits area [Ghisetti and Vezzani, 1982; Ghisetti, 1984 and 1992; Monaco and Tortorici 2000; among others], with a few, relatively small faults reported on the Sicilian side [Figure 2; Ghisetti, 1984; 1992], a few on the Calabrian side [such as the Mosorrofa fault, Figure 2; Ghisetti, 1992] and some offshore in the Straits [Figure 2; Selli, 1979; Guarnieri et al., 2004]. Major relevance is attributed to the NE- and NNE-trending structural systems, with the latter widely believed to have produced the magnitude 7.1 earthquake of 1908 [see Boschi et al., 1989; DISS Working Group, 2021; among others].

A detailed geological field survey, integrated by geomorphological analyses made on topographic maps and DTM, has allowed us to detect a NW-trending fault (which we call Trapani Stream Fault) corresponding to the clear change of HVSR data shown in Figure 5. For this fault our data show normal faulting and activity at least until Middle Pleistocene, with likely prosecution during Upper Pleistocene. Present-day activity cannot be excluded. The Trapani Stream Fault follows the Torrente Trapani valley in its northwesternmost detected segment and continues southeast-ward beneath the center of the town in the coastal area of the Straits (Figure 7).

We may use the results of Neri et al.'s [2021] analysis of low-magnitude seismicity recently occurred in the study area in order to attempt a preliminary comparison between the Trapani Stream Fault and the recent seismic activity. In the Figure 6 of Neri et al.'s paper, the only earthquake occurring in the sector of the Trapani Stream Fault is that indicated as n. 14. This earthquake, of magnitude $Mw = 3.6$, occurred on December 23, 2013, and was located at a depth of about 10 km beneath the Messina harbor area (see location and focal mechanism of this event redrawn in our Figure 10). The focal mechanism taken from Neri et al. [2021] indicates normal faulting with a significant lateral-slip component: the nodal planes are NW- and NE-trending, respectively (Figure 10). In order to make a very preliminary attempt to identify which of the two nodal planes may be the fault plane of this earthquake, we have joined for stress inversion the two quality controlled datasets of local earthquake focal mechanisms published by Neri et al. [2005] and Neri et al. [2021]. For the stress inversion, we have applied the Gephart and Forsyth's [1984] standard method on the mechanisms of earthquakes located in the Straits area (37.90°N-38.33°N, 15.50°E-15.84°E) at depths less than 18 km corresponding to the overriding plate in this subduction zone [Maesano et al., 2017; Orecchio et al., 2021]. The dataset of focal mechanisms used for inversion is reported in Table 1. The best model of stress obtained by inversion is shown in Figure 10. The solution indicates stress homogeneity (minimum average misfit of 4.2°), a fairly good constraint (see the 95% confidence limits) and appears very similar to that furnished by Neri et al. [2005]. The analysis of individual misfits of the nodal planes of the 2013 earthquake in Figure 10 with respect to the stress solution (made according to Gillard et al, 1996; Neri et al., 2005) reveals that the NW-trending nodal plane (misfit of 6.7°) is compatible with the best stress model, while the NE-trending one (misfit of 16.5°) is not. Our high-quality Bayesian location of the earthquake made using the local 3D velocity structure by Orecchio et al. [2011] and the Bayloc location method by Presti et al. [2004 and 2008] indicates that the epicenter is close to the SE-ward prolongation of the Trapani Stream Fault in the harbor of Messina.

On the other hand, the hypocentral depth of about 10 km introduces the unknown of the dip of the fault surface between the hypocenter and the ground surface, when trying to compare the earthquake with the Trapani Stream Fault. In addition, the nodal plane found to have acted as the fault plane is SW-ward dipping with hanging-wall located southwest of the same plane, and this would exclude the Trapani Stream Fault as the source of the

Date (yyyymmdd)	O.T. (hh:mm)	Lon (°E)	Lat (°N)	Depth (km)	strike (°)	dip (°)	rake (°)	Mw	Source
19081228	04:20	15.60	38.12	10.0	–65	208	55	7.0	Gasparini et al., 1985
19881107	14:26	15.84	38.09	16.4	80	200	85	3.4	Neri et al., 2003
19910907	05:39	15.50	37.96	8.4	–160	20	85	3.2	Neri et al., 2003
19920628	06:03	15.80	38.33	14.2	10	110	80	3.3	Frepoli and Amato, 2000
19940819	01:51	15.82	37.95	15.9	–80	110	50	3.0	Frepoli and Amato, 2000
20000308	09:38	15.75	38.23	13.3	–150	50	30	3.0	Neri et al., 2003
20050419	22:36	15.62	38.13	7.1	220	42	–10	3.1	D'Amico et al., 2010
20061006	21:16	15.56	38.09	11.0	33	51	–90	3.2	Neri et al., 2021
20080413	13:06	15.68	38.25	14.3	6	47	–36	2.8	Orecchio et al., 2014
20130303	23:39	15.83	38.12	8.0	237	57	–82	3.3	Totaro et al., 2016
20131223	04:20	15.56	38.19	11.0	48	67	–32	3.6	Neri et al., 2021
20180210	02:16	15.75	38.19	12.6	42	82	–41	3.6	Neri et al., 2021

Table 1. Date and origin time, hypocenter coordinates, fault parameters and moment magnitude of the earthquakes used for the stress inversion. The bibliographic source of each focal mechanism is also reported in the last column.

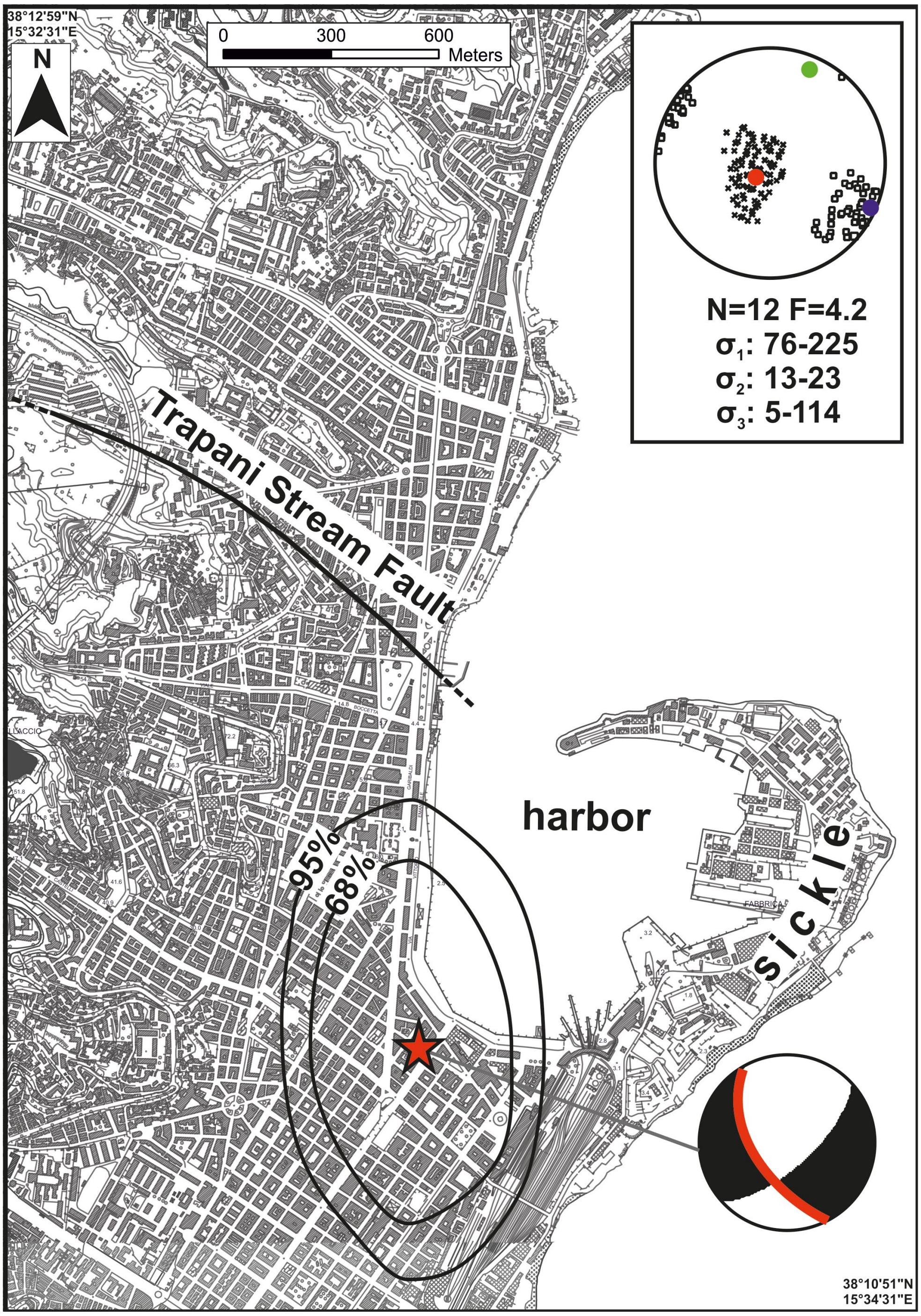

Figure 10. The figure shows the topographic map of the historic center of Messina. The black line indicates the Trapani Stream Fault detected in the present study on the basis of geophysical (HVSR), geological and geomorphological investigations. The red star indicates the epicenter of the Mw 3.6 earthquake occurred at about 10 km depth on 23 December 2013. The ellipses around the epicenter indicate the 68 and 95% confidence limits of the location estimated by the Bayloc Bayesian algorithm of Presti et al. [2004, 2008]. The waveform inversion focal mechanism of the same earthquake is also reported [from Neri et al., 2021]. The inset shows the orientations of the principal stress axes (lower hemisphere stereographic projection) estimated by inversion of the earthquake focal mechanisms of Table 1 (see text for details). Red, green, and blue dots indicate the orientations of the maximum (σ1), intermediate (σ2), and minimum (σ3) compressive stresses, respectively. Crosses and squares indicate the 95% confidence areas for the σ1 and σ3 axes, respectively. F is the average of the individual earthquake misfits with respect to the best model of stress found by inversion. N is the number of focal mechanisms used for stress inversion. The red nodal plane in the focal mechanism is that identified as the fault plane using the procedure by Gillard et al. [1996] and Neri et al. [2005].

earthquake. We have said in a previous section that a transverse (to the main NNE-SSW fault system) horst structure was detected by several authors in the Messina harbor area [Franchi, 1909; Ghisetti 1984]. The evident structural complexity of the specific study area leads us to consider that further and deeper investigations are needed to clarify relationships between the earthquake and the local faults and structures. In particular, the preliminary stress inversion performed in the present study needs to be updated (a) testing also other inversion algorithms and (b) attempting the improvement of the focal mechanism dataset with the inclusion of other good-quality focal solutions. In addition, there are other focal mechanisms in the Figure 6 of Neri et al. [2021], as well as the focal mechanism of the 1975 earthquake of magnitude 4.6 published by Gasparini et al. [1985], indicating (with their NW-trending nodal planes) the need of a wider analysis of the seismogenic attitude of the NW-SE fault system over the whole Straits area. This new analysis is being planned.

In conclusion, we offer clear evidence in the present study of a previously undetected fault crossing the center of the town of Messina from NW to SE, therefore roughly perpendicular to the strike of the main structural system widely believed to have generated the major earthquake of 1908. The new detected fault requires future deeper investigation to establish (a) if any lateral component of slip is to be considered in addition to clearly observed normal faulting, (b) its real extent, i.e. an eventual prosecution towards northwest and southeast, respectively, and (c) if the fault is a part of a larger system, such as the NW-SE Southern Tyrrhenian Fault System [Lentini and Carbone, 2014], or a minor structure eventually related to the activity of the deeper, 1908 earthquake source. The great relevance of the 1908 earthquake has, to date, comprehensibly limited the investigational efforts and the attention of the scientific community towards structural systems (and potential sources of earthquakes) different from the NNE-SSW one. Future research efforts in the Messina Straits area need to be expanded to a wider set of geostructural features and potentially seismogenic faults.

Acknowledgements. We thank the Editor and two anonymous reviewers for the critical reviews and constructive comments. This research has benefited from funding provided by PO-FESR 2014/2020, ID 08CT2790090212 Project 'HCH LowCostGeoEngineering Check'. We also thank the Geologist Di Nuzzo for providing HVSR data collected during recent surveys, and the Messina Municipality for furnishing the topographic 1:2.000 map and seismic microzoning and borehole data.

Data and sharing resources.

- Topographic map 1:10.000 used in this study can be downloaded from the data base of SITR, Sistema Informativo Territoriale Regionale following the link: www.sitr.regione.sicilia.it.
- HVSR analysis were performed using Grilla (https://moho.world/tromino/) and Geopsy (http://www.geopsy.org) softwares.

References

Aloisi, M., V. Bruno, F. Cannavò, L. Ferranti, M. Mattia, C. Monaco and M. Palano (2013). Are the Source Models of the M 7.1 1908 Messina Straits Earthquake Reliable? Insights from a Novel Inversion and a Sensitivity Analysis of Levelling Data, Geophys. J. Int., 192, 3, 1025-1041, doi:10.1093/gji/ggs062

Amodio Morelli, L., G. Bonardi, V. Colonna, D. Dietrich, G. Giunta, F. Ippolito, V. Liguori, S. Lorenzoni, A. Paglionico, V. Perrone, G. Piccarreta, M. Russo, P. Scandone, E. Zanettin-Lorenzoni and A. Zuppetta (1976). L'Arco Calabro-Peloritano nell'orogene Appenninico-Maghrebide, Mem. Soc. Geol. Ital., 17, 1-60.

Amoruso, A., L. Crescentini, G. Neri, B. Orecchio and R. Scarpa (2006). Spatial Relation between the 1908 Messina Straits Earthquake Slip and Recent Earthquake Distribution, Geophys. Res. Lett., 33, 17, doi:10.1029/2006GL027227

Amoruso, A., L. Crescentini and R. Scarpa (2002). Source Parameters of the 1908 Messina Straits, Italy, Earthquake from Geodetic and Seismic Data, J. Geophys. Res., 107, 4-1, doi:10.1029/2001JB000434

Argnani, A. (2022). Comment on the paper by Barreca et al.: "The Strait of Messina: Seismotectonics and the source of the 1908 earthquake", Earth-Sci. Rev., 226, 103961, doi:10.1016/j.earscirev.2022.103961

Bada, J.L., G. Belluomini, L. Bonfiglio, M. Branca, E. Burgio and L. Delitala (1991). Isoleucine epimerization ages of Quaternary Mammals of Sicily, Il Quaternario, 4, 5-11.

Bard, P. Y. (2005). Guidelines for the implementation of the H/V spectral ratio technique on ambient vibrations: measurements, processing, and interpretations. SESAME European research project. WP12, deliverable D23.12, 2004; available at: http://sesame.geopsy.org/Delivrables/Del-D23-HV_User_Guidelines.pdf

Barreca, G., F. Gross, L. Scarfì, M. Aloisi, C. Monaco and S. Krastel (2021). The Strait of Messina: Seismotectonics and the Source of the 1908 Earthquake, Earth-Sci. Rev., 218, 103685, doi:10.1016/j.earscirev.2021.103685

Barrier, P. (1986). Évolution paléogeographique du détroit de Messine au Pliocène et au Pléistocène, Giornale di Geologia, 48, 1-2, 7-24.

Bonfiglio, L., D. Violanti and M. Marchetti (1991). Il substrato neogenico della Formazione delle Ghiaie di Messina sulla sponda siciliana dello Stretto, Mem. Soc. Geol. Ital., 47, 27-37.

Bonini, L., D. Di Bucci, G. Toscani, S. Seno and G. Valensise (2011). Reconciling Deep Seismogenic and Shallow Active Faults through Analogue Modelling: the Case of the Messina Straits (Southern Italy), J. Geol. Soc., 168, 1, 191-199, doi:10.1144/0016-76492010-055

Bonnefoy-Claudet, S., F. Cotton and P. Y. Bard (2006a). The nature of noise wavefield and its applications for site effects studies: a literature review; Earth-Sci. Rev., 79, 3, 205-227, doi: 10.1016/j.earscirev.2006.07.004

Bonnefoy-Claudet, S., C. Cornou, P. Y. Bard, F. Cotton, P. Moczo, J. Kristek and D. Fäh (2006b). H/V ratio: a tool for site effects evaluation. Results from 1-D noise simulations, Geophys. J. Int., 167, 2, 827-837, doi: 10.1111/j.1365-246X.2006.03154.x

Boschi, E., D. Pantosti and G. Valensise (1989). Modello di sorgente per il terremoto di Messina del 1908 ed evoluzione recente dell'area dello Stretto. Roma, Atti VIII Convegno GNGTS, 245-258.

Bottari, A., E. Carapezza, M. Carapezza, P. Carveni, F. Cefali, E. L. Giudice and C. Pandolfo (1986). The 1908 Messina Strait earthquake in the regional geostructural framework, J: Geodyn., 5, 3-4, 275-302, doi:10.1016/0264-3707(86)90010-4

Capuano, P., G. De Natale, P. Gasparini, F. Pingue and R. Scarpa (1988). A Model for the 1908 Messina Straits (Italy) Earthquake by Inversion of Levelling Data, Bull. Seism. Soc. Am., 78, 6, 1930-1947.

Castellaro, S. and F. Mulargia (2009). The effect of velocity inversions on H/V, Pure Appl. Geophys., 166, 4, 567-592, Doi: 10.1007/s00024-009-0474-5

Catalano, S. and A. Cinque (1995). L'evoluzione neotettonica dei Peloritani settentrionali (Sicilia nord-orientale): il contributo di una analisi geomorfologica preliminare. Università di Camerino (Editor), Studi geologici camerti, n. speciale, 1995, 113-123.

Catalano, S. and G. De Guidi (2003). Late Quaternary uplift of northeastern Sicily: relation with the active normal faulting deformation, J. Geodyn., 36, 4, 445-467, doi:10.1016/S0264-3707(02)00035-2

Catalano, S., G. De Guidi, C. Monaco, G. Tortorici and L. Tortorici (2008). Active faulting and seismicity along the Siculo-Calabrian Rift Zone (Southern Italy), Tectonophysics, 453, 1-4, 177-192, doi:10.1016/j.tecto.2007.05.008.

Comerci, V., E. Vittori, A. M. Blumetti, E. Brustia, P. Di Manna, L. Guerrieri, M. Lucarini and L. Serva (2015). Environmental effects of the December 28, 1908, Southern Calabria-Messina (Southern Italy) earthquake, Natural Hazards, 76, 1849-1891, doi: 10.1007/s11069-014-1573-x

Del Ben, A., C. Gargano and R. Lentini (1996). Ricostruzione strutturale e stratigrafica dell'area dello Stretto di Messina mediante analisi comparata dei dati geologici e sismici, Mem. Soc. Geol. It., 51, 703-717.

De Natale, G. and F. Pingue (1991). A Variable Slip Fault Model for the 1908 Messina Straits (Italy) Earthquake, by Inversion of Levelling Data, Geophys, J. Int., 104, 1, 73-84, doi:10.1111/j.1365-246X.1991.tb02494.x

Di Giulio, G., R. de Nardis, P. Boncio, G. Milana, G. Rosatelli, F. Stoppa and G. Lavecchia (2016). Seismic response of a deep continental basin including velocity inversion: the Sulmona intramontane basin (Central Apennines, Italy), Geophys. J. Int., 204, 1, 418-439, Doi:10.1093/gji/ggv444

DISS Working Group (2021). Database of Individual Seismogenic Sources (DISS), Version 3.3.0: A compilation of potential sources for earthquakes larger than M 5.5 in Italy and surrounding areas. Istituto Nazionale di Geofisica e Vulcanologia (INGV). https://doi.org/10.13127/diss3.3.0

Doglioni, C., M. Ligi, D. Scrocca, S. Bigi, G. Bortoluzzi, E. Carminati, M. Cuffaro., F. D'Oriano, V. Forleo, F. Muccini and F. Riguzzi. (2012). The tectonic puzzle of the Messina area (Southern Italy): Insights from new seismic reflection data, Sci. Rep., 2, 1, 1-9.

Faccenna, C., P. Molin, B. Orecchio, V. Olivetti, O. Bellier, F. Funiciello, L. Minelli, C. Piromallo and A. Billi (2011). Topography of the Calabria Subduction Zone (Southern Italy): Clues for the Origin of Mt. Etna, Tectonics, 30, TC1003, doi:10.1029/2010TC002694

Fäh, D., F. Kind and D. Giardini (2001) A theoretical investigation of average H/V ratios, Geophys. J. Int., 145, 535-549, doi: 10.1046/j.0956-540x.2001.01406.x

Ferranti, L., C. Monaco, D. Morelli, F. Antonioli and L. Maschio (2008). Holocene activity of the Scilla Fault, Southern Calabria: Insights from coastal morphological and structural investigations, Tectonophysics, 453, 1-4, 74-93, doi:10.1016/j.tecto.2007.05.006

Ferrara, V. (1999). Vulnerabilità all'inquinamento degli acquiferi dell'area peloritana (Sicilia nord-orientale). Studi sulla vulnerabilità degli acquiferi 14, Pubblicazione GNDCI-CNR n.1946, Pitagora Editrice, Bologna.

Finetti, I.R. (2008). Geophysical Exploration Contribution to the Understanding of Messina Straits Tectono-Dynamics and 1908 Earthquake, Seismogenesis. Environmental Semeiotis, 1, 2, 278-293.

Finetti, I.R., F. Lentini, S. Carbone, S Catalano and A. Del Ben (1996). Il sistema appenninico meridionale-arco calabro-Sicilia: studio geologico-geofisico, Boll. Soc. Geol. It., 115, 529-559.

Finetti, I.R., F. Lentini, S. Carbone, A. Del Ben, A. Di Stefano, E. Forlin, P. Gurnieri, M. Pipan, and A. Prizzon (2005). Geological outline of Sicily and lithospheric tectono-dinamics of its Tyrrhenian Margin from new CROP seismic data, in CROP Deep Seismic exploration of the Mediterranean Region. Spec. Vol. Elsevier, chapt. 15, 319-376.

Franchi, S. (1909). Il terremoto del 28 dicembre 1908 a Messina, in rapporto alla natura del terreno ed alla riedificazione della città, Boll. Comit. Geol. Ital, 111-157.

Gargano, C. (1994). Carta geologica di Messina e del settore nord-orientale dei Monti Peloritani. Università di Catania, Istituto di Geologia e Geofisica, scala 1:25.000. S.EL.CA., Firenze.

Gasparini, C., G. Iannaccone and R. Scarpa (1985). Fault-plane solutions and seismicity of the Italian peninsula, Tectonophysics, 117, 1/2, 59-78, doi: 10.1016/0040-1951(85)90236-7

Gephart, J. W. and D. W. Forsyth (1984). An improved method for determining the regional stress tensor using earthquake focal mechanism data: application to the San Fernando earthquake sequence, J. Geophys. Res.: Solid Earth, 89, B11, 9305-9320. Doi: 10.1029/JB089iB11p09305

Ghisetti, F. (1979). Evoluzione neotettonica dei principali sistemi di faglie della Calabria centrale, Bollettino della Società Geologica Italiana, 98, 25, 387-430.

Ghisetti, F. (1984). Recent deformations and the seismogenic source in the Messina Strait (southern Italy), Tectonophysics, 109, 191-208. doi:10.1016/0040-1951(84)90140-9

Ghisetti, F. (1992). Fault Parameters in the Messina Strait (Southern Italy) and Relations with the Seismogenic Source, Tectonophysics, 210, 1-2, 117-133. doi:10.1016/0040-1951(92)90131-o

Ghisetti, F. and L. Vezzani (1982). Different styles of deformation in the Calabrian arc (southern Italy): implications for a seismotectonic zoning, Tectonophysics, 85, 3-4, 149-165, https://doi.org/10.1016/0040-1951(82)90101-9

Gillard, D., M. Wyss and P. Okubo (1996). Type of faulting and orientation of stress and strain as a function of space and time in Kilauea's south flank, Hawaii, J. Geophys. Res., 101, 16025-16042, Doi: 10.1029/96JB00651

Guarnieri, P., A. Di Stefano, S. Carbone, F. Lentini and A. Del Ben (2004). A multidisciplinary approach to the reconstruction of the Quaternary evolution of the Messina Strait (with Geological Map of the Messina Strait 1:25.000 scale), in Mapping Geology in Italy Pasquarè, G., Venturini, C. (Editor), APAT, Roma, 45-50.

Guarnieri, P. (2006). Plio-Quaternary segmentation of the South Tyrrhenian Forearc basin, Int. J. Earth Sci. (Geol. Rundsch.) 95, 107-118. Doi: doi.org/10.1016/j.geomorph.2007.06.013

Guarnieri, P. and C. Pirrotta (2008). The response of drainage basins to the late Quaternary tectonics in the Sicilian side of the Messina Strait (NE Sicily), Geomorphology, 95, 3-4, 260-273. Doi:10.1016/j.geomorph.2007.06.013

Ibs-von Seht, M. and J. Wohlenberg (1999). Microtremor measurements used to map thickness of soft sediments, Bull. Seismol. Soc. Am., 89, 1, 250-259, doi: 10.1785/BSSA0890010250

Lachet, C. and P. Y. Bard (1994). Numerical and Theoretical Investigations on the Possibilities and Limitations of Nakamura's Technique, J. Phys. Earth, 42, 5, 377-397, doi: 10.4294/jpe1952.42.377

Lentini, F. (1999). Carta geologica della Provincia di Messina, scala 1:50.000, 3 fogli. S.EL.CA. (Ed.), Firenze.

Lentini, F. and S. Carbone (2014). Geologia della Sicilia. Mem. Descr. Carta Geol. d'It. XCV, 7-414 figg. 533, tabb. 5; Tavv. 5.

Lentini, F., S. Carbone and S. Catalano (1994). Main structural domains of the central mediterranean region and their tectonic evolution, Boll. Geofis. Teor. Appl., 36, 141-144, 103-125.

Lentini, F., S. Catalano and S. Carbone (2000). Note Illustrative della Carta Geologica della Provincia di Messina, scala 1:50.000. S.EL.CA. (Ed.), Firenze.

Maesano, F. E., M. M. Tiberti and R. Basili (2017). The Calabrian Arc: threedimensional modelling of the subduction interface, Sci. Rep. 7, 8887, doi:10.1038/s41598-017-09074-8

Mariucci, M.T. and P. Montone (2020). Database of Italian present-day stress indicators, IPSI 1.4. Sci Data 7, 298, https://doi.org/10.1038/s41597-020-00640-w

Meschis, M., G. P. Roberts, Z. K. Mildon, J. Robertson, A. M. Michetti, and J. P. Faure Walker (2019). Slip on a mapped normal fault for the28th December 1908 Messina earthquake (Mw 7.1) in Italy, Scientific Rep., 9, 1, 6481. doi: 10.1038/s41598-019-42915-2.

Monaco C., G. Barreca and A. Di Stefano (2017). Quaternary marine terraces and fault activity in the northern mainland sectors of the Messina Strait (southern Italy), It. J. Geosci., 136, 3, 337-346, Doi:10.3301/IJG.2016.10

Monaco, C. and L. Tortorici (2000). Active Faulting in the Calabrian Arc and Eastern Sicily, J. Geodyn., 29, 3-5, 407-424, doi:10.1016/S0264-3707(99)00052-6

Municipality of Messina (2014). Microzonazione sismica di I livello del Comune di Messina.

Nakamura, Y. (1989). A method for dynamic characteristics estimation of subsurface using microtremor on the ground surface, Quarterly Report Railway Tech. Res. Inst., 30, 1, 25-30.

Neri, G., G. Barberi, G. Oliva and B. Orecchio (2004). Tectonic stress and seismogenic faulting in the area of the 1908 Messina earthquake, south Italy, Geophys. Res. Lett., 31, 10, L10602, doi:10.1029/2004GL019742

Neri, G., G. Barberi, G. Oliva and B. Orecchio (2005). Spatial variations of seismogenic stress orientations in Sicily, south Italy, Phys. Earth Planet. In., 148, 175-191, doi:10.1016/j.pepi.2004.08.009

Neri, G., G. Barberi, B. Orecchio and A. Mostaccio (2003). Seismic strain and seismogenic stress regimes in the crust of the southern Tyrrhenian region, Earth Planet. Sci. Lett., 213, 1-2, 97-112, doi.:10.1016/S0012-821X(03)00293-0

Neri, G., A. M. Marotta, B. Orecchio, D. Presti, C. Totaro, R. Barzaghi and A. Borghi (2012). How lithospheric subduction changes along the Calabrian Arc in southern Italy: geophysical evidences, Int. J. Earth Sci., 101, 1949-1969, doi:10.1007/s00531-012-0762-7

Neri, G., G. Oliva, B. Orecchio and D. Presti (2006). A possible seismic gap within a highly seismogenic belt crossing Calabria and eastern Sicily, Italy, Bull. Seismol. Soc. Am. 96, 1321-1331, doi:10.1785/0120050170

Neri, G., B. Orecchio, D. Presti, S. Scolaro and C. Totaro. (2021). Recent seismicity in the area of the major, 1908 Messina Straits earthquake, south Italy, Front. Earth Sci., 9, 667501, doi:10.3389/feart.2021.667501

Neri, G., P. Pino, P. Presti, S. Scolaro, S. D'Amico, C. Navarra, B. Orecchio and A. Torre (2022). About the role of NW-trending fault systems in the Messina Straits area. 40th National Conference of the GNGTS, Trieste, 27-29 June 2022

Nocquet, J.M. (2012). Present-day Kinematics of the Mediterranean: A Comprehensive Overview of GPS Results, Tectonophysics 579, 220-242, doi:10.1016/j.tecto.2012.03.037

Nogoshi, M. and T. Igarashi (1971). On the amplitude characteristics of microtremor (part 2), J. Seismol. Soc. Japan, 24, 26-40.

Orecchio, B., G. Neri, D. Presti, S. Scolaro and C. Totaro (2021). Seismic deformation styles in the upper and lower plate domains of the Calabrian subduction zone, south Italy, J. Geodyn., 145, 101847, doi: 10.1016/j.jog.2021.101847

Orecchio, B., D. Presti, C. Totaro, I. Guerra and G. Neri (2011). Imaging the velocity structure of the Calabrian Arc region (south Italy) through the integration of different seismological data, Boll. Geofis. Teor. Appl., 52, 625-638, doi:10.4430/bgta0023

Pino, N.A., M. Palano and G. Ventura (2021). Comment on the paper by Barreca et al.: "The Strait of Messina: Seismotectonics and the source of the 1908 earthquake", Earth-Sci. Rev., 223, 103865, doi: 10.1016/j.earscirev.2021.103865

Polonia, A., L. Torelli, A. Artoni, M. Carlini, C. Faccenna, L. Ferranti, L. Gasperini, R. Govers, D. Klaeschen, C. Monaco, G. Neri, N. Nijholt, B. Orecchio and R. Wortel (2016). The Ionian and Alfeo-Etna Fault Zones: New Segments of an Evolving Plate Boundary in the central Mediterranean Sea?, Tectonophysics, 675, 69-90, doi:10.1016/j.tecto.2016.03.016

Presti, D., A. Billi, B. Orecchio, C. Totaro, C. Faccenna and G. Neri (2013). Earthquake focal mechanisms, seismogenic stress, and seismotectonics of the Calabrian Arc, Italy, Tectonophysics, 602, 153-175, doi:10.1016/j.tecto.2013.01.030

Presti, D., B. Orecchio, G. Falcone and G. Neri (2008). Linear versus non-linear earthquake location and seismogenic fault detection in the southern Tyrrhenian Sea, Italy, Geophys, J. Int., 172, 607-618, doi:10.1111/j.1365-246x.2007.03642.x

Presti, D., C. Troise and G. De Natale (2004). Probabilistic location of seismic sequences in heterogeneous media, Bull. Seismol. Soc. Am., 94, 2239-2253, doi:10.1785/0120030160

Rovida, A., M. Locati, R. Camassi, B. Lolli, P. Gasperini and A. Antonucci (2022). Italian Parametric Earthquake Catalogue (CPTI15), version 4.0. Istituto Nazionale di Geofisica e Vulcanologia (INGV). https://doi.org/10.13127/CPTI/CPTI15.4

Scolaro, S., P. Pino, S. D'Amico, B. Orecchio, D. Presti, A. Torre, C. Totaro, D. Farruggia and G. Neri (2018). Ambient noise measurements for preliminary microzoning studies in the city of Messina, Sicily, Ann. Geoph., 61, 1-58, doi: 10.4401/ag-7711

Schick, R. (1977). Eine seimotektonische Bearbeitung des Erdbedens von Messina aus dem Jahre 1908, Geol. Jb. E-11, 3-74.

Selli, R. (1979). Geologia e sismotettonica dello Stretto di Messina. Convegno su: L'attraversamento dello Stretto di Messina e la sua fattibilità, 4-6 Luglio 1978. Atti Acc. Naz. Lincei, 43, 119-154.

Selli, R., P. Colantoni, A. Fabri, S. Rossi, A. M. Borsetti and P. Gallignani (1978). Marine Geological Investigations on the Messina Strait and its approaches, Giornale di Geologia, 42, 2.

Servizio Geologico di Italia (2008). Carta Geologica d'Italia in scala 1:50.000, Foglio 601 Messina, Reggio Calabria, Coordinatore F. Lentini. APAT/Regione Siciliana/D.S.G.-Università di Catania. ISPRA.

Società Stretto di Messina (2011). Progetto definitivo del Ponte sullo Stretto di Messina. Società Stretto di Messina, Roma.

Tortorici, L., C. Monaco, C. Tansi and O. Cocina (1995). Recent and active tectonics in the Calabrian Arc (southern Italy), Tectonophysics, 243, 37-55, doi:10.1016/0040-1951(94)00190-k

Totaro, C., B. Orecchio, D. Presti, S. Scolaro and G. Neri (2016). Seismogenic Stress Field Estimation in the Calabrian Arc Region (South Italy) from a Bayesian Approach, Geophys. Res. Lett., 43, 17, 8960-8969. doi:10.1002/2016GL070107

Wathelet, M., J. L. Chatelain, C. Cornou, G. D. Giulio, B. Guillier, M. Ohrnberger and A. Savvaidis (2020). Geopsy: A user-friendly open-source tool set for ambient vibration processing, Seismol. Res. Lett., 91, 3, 1878-1889, Doi: 10.1785/022019036

***CORRESPONDING AUTHOR: Silvia SCOLARO**,

Department of Engineering, University of Messina and Department of Mathematics, Computer Sciences, Physics, and Earth Sciences, University of Messina

e-mail: silscolaro@unime.it